

# Chiral and $U(1)$ axial symmetry restoration in linear sigma models with two quark flavors

Stefan Michalski\*

*Theoretische Physik IIIb  
Institut für Physik  
Universität Dortmund  
D-44221 Dortmund, Germany*

## Abstract

We study the restoration of chiral symmetry in linear sigma models with two quark flavors. The models taken into consideration have a  $U(2) \times U(2)$  and an  $O(N)$  internal symmetry. The physical mesons of these models are  $\sigma$ , pion,  $\eta$  and  $a_0$  where the latter two are not present in the  $O(N)$  model. Including two-loop contributions through sunset graphs we calculate the temperature behavior of the order parameter and the masses for explicit chiral symmetry breaking with and without a  $U(1)$  axial anomaly. Decay threshold effects introduced by the sunset graphs alter the temperature dependence of the condensate and consequently that of the masses as well. Chiral symmetry tends to be restored at higher temperatures in the two-loop approximation than in the Hartree-Fock approximation. To model a restoration of the  $U(1)$  axial symmetry we imply a temperature-dependent anomaly parameter that sharply drops at about 175 MeV. This triggers the restoration of chiral symmetry before the full symmetry is restored at about 300 MeV.

---

\*e-mail: stefan.michalski@uni-dortmund.de

# 1 Introduction

The Lagrangian of massless quantum chromodynamics (QCD) with  $N_f$  quark flavors has a chiral  $SU(N_f)_L \times SU(N_f)_R \times U(1)_A \times U(1)_V$  symmetry. A chiral quark condensate  $\langle \bar{q}q \rangle \approx (300 \text{ MeV})^3$  spontaneously breaks the  $SU(N_f)_A \times U(1)_A \simeq U(N_f)_A$  part of the symmetry and generates  $N_f^2$  Goldstone bosons. Apart from that there is also a violation of the  $U(1)_A$  symmetry by instantons [1, 2, 3] giving mass to one of the Goldstone bosons. The  $U(1)_V$  (vector) symmetry represents baryon number conservation, is always fulfilled and therefore will not be considered here. Adding mass terms like  $m_q \bar{q}q$  to the QCD Lagrangian breaks the symmetry explicitly and gives all Goldstone bosons a mass, making them pseudo-Goldstone bosons. Chiral symmetry is expected to be restored at temperatures of the order of  $\langle \bar{q}q \rangle^{1/3} \approx 300 \text{ MeV}$ . Recently, lattice QCD has been able to determine the critical temperature where chiral symmetry is restored. For three flavors it has been found to be in the vicinity of 155 MeV while for two flavors it is about 170 MeV [4] for a vanishing quark chemical potential. In spite of being a challenging first-principle approach to QCD, lattice calculation suffer from technical difficulties for small quark masses [5] or for a chemical potential larger than the temperature [6].

A different nonperturbative approach to QCD is the construction of low-energy effective theories of hadrons with the same chiral symmetry. The color degrees of freedom are integrated out so that the low-energy behavior of QCD is determined by the lightest hadrons which are scalar and pseudoscalar mesons with, in general, light quark content. These particles can be found in linear sigma models [7]. Since they have the same symmetries as the underlying fundamental theory, QCD, they can be used to study the dynamics of phase transitions at finite temperature.

These models cannot be solved analytically so one has to make use of approximations. One problem arising at finite temperature is the breakdown of perturbation theory. At a temperature  $T$ , a (perturbative) expansion in powers of a coupling  $g$  yields a new mass scale  $gT$  that occurs in the denominators of loop graphs and cancels powers of the coupling constant in the perturbation expansion [8, 9, 10, 11]. So, terms of all orders of the coupling must be taken into account via resummation to avoid these unwanted cancellations. The resummation scheme we apply here is the so-called *two-particle point-irreducible* (2PPI) effective action first introduced by Verschelde and Coppens [12]. Up to the level of the Hartree-Fock approximation it is identical to the *two-particle irreducible* (2PI) effective action formalism by Cornwall, Jackiw and Tomboulis [13].

Linear sigma models with a  $U(N_f) \times U(N_f)$  symmetry and two to four quark flavors have been studied in the Hartree-Fock (HF) approximation within the last more than 25 years [14, 15, 16, 17]. The  $O(N)$  model has received even greater attention. It has been analyzed using different resummation techniques, where various authors used local resummations [8, 18, 19, 20, 21, 22, 23, 24, 25], while, nowadays, nonlocal schemes, like the two-particle irreducible effective action [13], have become popular as well [26, 27, 28, 29, 30]. Furthermore, renormalization has become a heavily studied issue in this context [31, 32, 33, 34, 35].

The Hartree–Fock (HF) approximation as well as the two-loop approximation of the 2PPI effective action violate Goldstone’s theorem because the formalism’s variational parameter associated to the Goldstone boson mass achieves finite values at temperatures above zero [19, 25]. This problem can be overcome either by looking at the external (or physical) propagators — the derivatives of the one-particle (1PI) effective action — or by a construction described in Ref. [36]. For a renormalization group invariant approach see recent work of Destri and Sartirana [37, 38].

The  $U(N_f)_L \times U(N_f)_R$  linear sigma model contains two  $U(N_f)$  isospin multiplets — a scalar and a pseudoscalar one — each of which is decomposed into an isosinglet and an isospin  $(N_f^2 - 1)$  multiplet. For two flavors and unbroken isospin symmetry ( $m_u = m_d$ ) we obtain four different mesons in the model,  $\sigma$  [called  $f_0(600)$  nowadays] with an isotriplet of (identical)  $a_0$  bosons in the scalar sector, and  $\eta$  with three pions in the pseudoscalar sector. The  $O(N)$  linear sigma model only consists of a  $\sigma$  meson and  $N - 1$  pions and is, for  $N = N_f^2 = 4$ , a limiting case of the  $U(2)_L \times U(2)_R$  model.

This article is organized as follows. In Sections 2 and 3 we describe the  $U(2)_L \times U(2)_R$  and the  $O(N)$  linear sigma model and their pattern of symmetry breaking. Section 4 deals with parameter fixing and numerical results in both models. Finally, in Section 5 we draw our conclusions and give an outlook. There is also an Appendix in which more details about the computation of the effective action of the  $U(2)_L \times U(2)_R$  model are given.

## 2 The $U(2)_L \times U(2)_R$ linear sigma model

### 2.1 Classical action

The Lagrangian of the  $U(N_f)_R \times U(N_f)_L$  linear sigma model is given by

$$\begin{aligned} \mathcal{L}[\Phi] = & \text{Tr} (\partial_\mu \Phi^\dagger \partial^\mu \Phi - m^2 \Phi^\dagger \Phi) - \lambda_1 [\text{Tr} (\Phi^\dagger \Phi)]^2 - \lambda_2 \text{Tr} [(\Phi^\dagger \Phi)^2] \\ & + c[\det \Phi + \det \Phi^\dagger] + \text{Tr} [H(\Phi + \Phi^\dagger)] . \end{aligned} \quad (1)$$

The field  $\Phi$  is a complex  $N_f \times N_f$  matrix containing the scalar and pseudoscalar mesons,

$$\Phi = T_a(\sigma_a + i\pi_a). \quad (2)$$

Here  $\sigma_a$  are the scalar fields with  $J^P = 0^+$  while  $\pi_a$  denotes the pseudoscalar ones with  $J^P = 0^-$ . The last term in the Lagrangian (1) breaks the symmetry explicitly,

$$H = T_a h_a , \quad (3)$$

where  $h_a$  are external fields.  $T_a$  are the generators of the group  $U(N_f)$  such that  $\text{Tr} (T_a T_b) = \delta_{ab}/2$ . The  $U(N_f)$  algebra is fulfilled

$$[T_i, T_j] = if_{ijk} T_k \quad (4a)$$

$$\{T_i, T_j\} = d_{ijk} T_k \quad (4b)$$

where  $f_{ijk}$  and  $d_{ijk}$  are the usual antisymmetric and symmetric structure constants of  $SU(N_f)$  and  $i, j, k = 1, \dots, N_f^2 - 1$ . The additional structure constants for  $U(N_f)$  are

$$f_{ab0} = 0, \quad d_{ab0} = \sqrt{\frac{2}{N_f}} \delta_{ab} \quad (4c)$$

with  $a, b, c = 0, \dots, N_f^2 - 1$ .

In the following we will deal only with the case  $N_f = 2$  which reduces the structure constants to

$$f_{ijk} = \varepsilon_{ijk} \quad \text{and} \quad d_{ijk} = 0 \quad \text{for} \quad i, j, k \in \{1, 2, 3\}. \quad (5)$$

The usual identification of the physical bosons for  $N_f = 2$  is (see, *e.g.*, Ref. [14])

$$\Phi = \frac{1}{\sqrt{2}} \begin{pmatrix} \frac{1}{\sqrt{2}}(\sigma + a_0^0) & a_0^+ \\ a_0^- & \frac{1}{\sqrt{2}}(\sigma - a_0^0) \end{pmatrix} + \frac{i}{\sqrt{2}} \begin{pmatrix} \frac{1}{\sqrt{2}}(\eta + \pi^0) & \pi^+ \\ \pi^- & \frac{1}{\sqrt{2}}(\eta - \pi^0) \end{pmatrix}. \quad (6)$$

Since isospin symmetry is left untouched the masses of all particles of one isovector are identical, *i.e.*,  $m_{a_0^0} = m_{a_0^\pm}$  and  $m_{\pi^0} = m_{\pi^\pm}$ .

## 2.2 Breaking the symmetry

The first three terms of the Lagrangian (1) are invariant under the group  $U(2)_L \times U(2)_R \simeq SU(2)_V \times SU(2)_A \times U(1)_A \times U(1)_V$ . The  $U(1)_V$  vector symmetry reflects baryon number conservation of QCD. We will not deal with this symmetry in this paper for it is always conserved. Chiral symmetry is spontaneously broken if the vacuum expectation value of the field  $\Phi$  does not vanish

$$\langle \Phi \rangle = T_a \phi_a. \quad (7)$$

The vacuum should be of even parity, so only  $\phi_a = \langle \sigma_a \rangle$  is allowed. According to a theorem by Vafa and Witten [39] global vector-like symmetries (isospin, baryon number) cannot be broken spontaneously. So, the remaining symmetry must be, at least,  $SU(2)_V$ . Spontaneously breaking  $SU(2)_A \times U(1)_A$  yields four Goldstone bosons,  $\eta$  and three pions. The determinants in the Lagrangian (1) break the  $U(1)_A$  symmetry explicitly which represents the  $U(1)$  axial anomaly [1] whose strength is given here by the constant  $c$ . This anomaly makes the isosinglet Goldstone boson  $\eta$  massive. The remaining  $SU(2)_V$  symmetry (of three pions) stays intact if we assume the masses of the up and down quark to be equal. So the vacuum expectation value is

$$\langle \Phi \rangle = T_0 \phi_0 = \frac{1}{2} \phi_0 \mathbf{1} \quad (8)$$

and thus points only in the 0-direction. Finally, the last term in the Lagrangian (1) explicitly breaks chiral symmetry and makes also the pions massive. It resembles the mass terms in the QCD Lagrangian where here  $H$  corresponds to the quark mass matrix and

$\Phi$  to the quark condensate. We will only deal with the case  $h_0 \neq 0$  and keep the  $SU(2)$  isospin symmetry ( $m_u = m_d$ ) conserved so that  $h_3 = 0$ .

With rising temperature we expect the chiral  $SU(2)_V \times SU(2)_A \simeq SU(2)_L \times SU(2)_R$  symmetry to be restored so that the chiral partners ( $\sigma$  and  $\pi$ ,  $\eta$  and  $a_0$ ) become degenerate in mass. A violation of the axial  $U(1)$  symmetry is inherent to the linear sigma model since its strength is directly given by one of the model's parameters. The restoration of this symmetry can only be modelled in a phenomenological way by making  $c$  temperature-dependent, *e.g.*, go down with rising  $T$ . For  $c \rightarrow 0$  we expect the  $\eta$  mass to become identical to the pion mass above a certain temperature so that there is a full  $U(2)_A$  symmetry in the pseudoscalar sector. And, finally, for a vanishing order parameter, all four masses are expected to become degenerate at temperatures above  $\langle \bar{q}q \rangle^{1/3} \approx 300$  MeV.

## 2.3 Effective action

We compute the effective action using the 2PPI formalism [12, 19, 24, 25]. We include all graphs up to two loops as shown in Fig. 1. The reader is referred to the Appendix for details of the computation. Here, we will only give the final result for the effective potential:

$$V_{\text{eff}}(M^2, \phi_0) = V_{\text{cl}}(\phi_0) + V_{\text{db}}(M^2, \phi_0) + V_q^{2\text{PPI}}(M^2, \phi_0) . \quad (9)$$

It is a function of the masses  $M_\sigma^2$ ,  $M_\pi^2$ ,  $M_\eta^2$  and  $M_{a_0}^2$  (denoted by  $M^2$  for brevity) and the condensate  $\phi_0$ . The classical part is

$$V_{\text{cl}}(\phi_0) = \frac{1}{2}(m^2 - c)\phi_0^2 + \left( \frac{\lambda_1}{4} + \frac{\lambda_2}{8} \right) \phi_0^4 - h_0 \phi_0 . \quad (10)$$

The quantum part  $V_q$  contains all *two-particle point-irreducible*<sup>2</sup> (2PPI) graphs that can be made of the vertices of the shifted Lagrangian except for the double bubbles which will be taken care of by  $V_{\text{db}}$ . The propagators within these graphs are defined by an effective mass and have the Euclidean form

$$G_*(p) = \frac{1}{p^2 + M_*^2} .$$

Here, we only take into account 2PPI graphs with one and two loops which leads to

$$\begin{aligned} V_q^{2\text{PPI}}(M^2, \phi_0) = & \frac{1}{2} \ln \det(\partial^2 + M_\sigma^2) + \frac{1}{2} \ln \det(\partial^2 + M_\eta^2) \\ & + \frac{3}{2} \ln \det(\partial^2 + M_{a_0}^2) + \frac{3}{2} \ln \det(\partial^2 + M_\pi^2) \\ & + V_{\text{sunsets}}(M^2, \phi_0) \end{aligned} \quad (11)$$

---

<sup>2</sup>Graphs that do not fall apart if two lines meeting at the same vertex are cut.

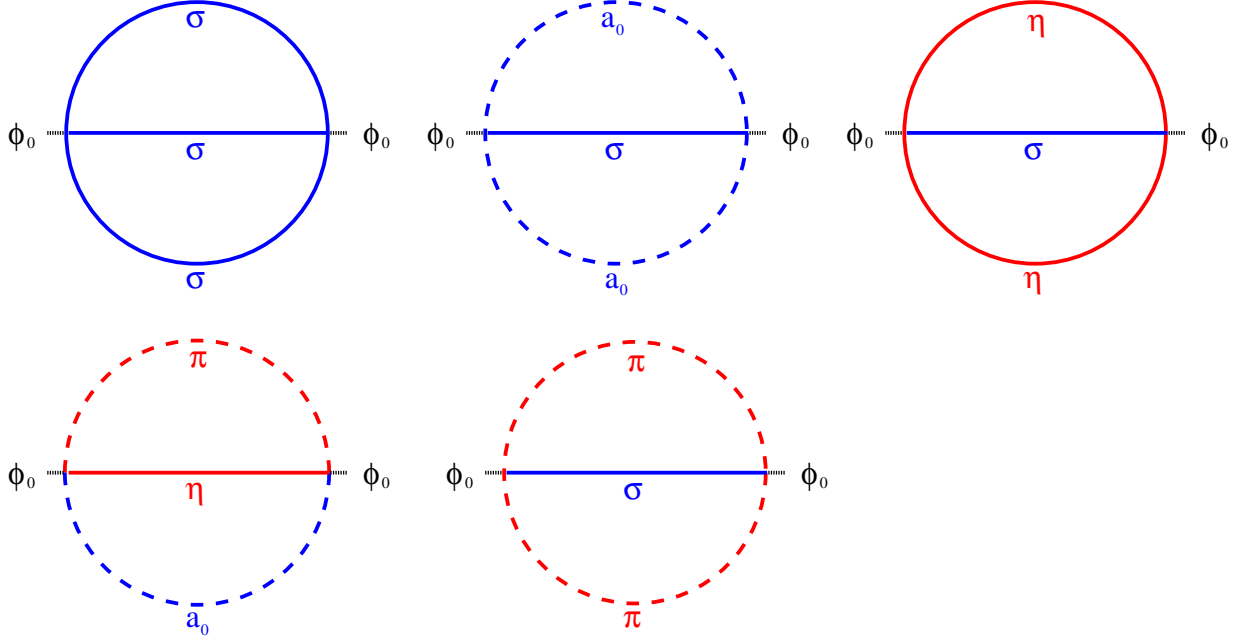


Figure 1: The sunset graphs as in Eq. (12). Scalars are drawn in blue, pseudoscalars in red. Dashed lines represent isotriplets while solid lines are used for isosinglets.

Using the trilinear part of the shifted Lagrangian  $\mathcal{L}_3$  (A4) we find the sunset contribution (note the minus sign)

$$V_{\text{sunset}}(M^2, \phi_0) = -\phi_0^2 \left[ \left( \lambda_1 + \frac{3}{2}\lambda_2 \right)^2 (3 S_{\sigma\sigma\sigma} + 3 S_{\sigma a_0 a_0} + S_{\sigma\eta\eta}) + \left( \lambda_1 + \frac{\lambda_2}{2} \right)^2 S_{\sigma\pi\pi} + \frac{3}{2}\lambda_2^2 S_{a_0\eta\pi} \right], \quad (12)$$

where  $S_{ijk}$  denotes the sunset graph made of the propagators of the particles  $i$ ,  $j$  and  $k$ . A graphical representation of these contributions can be found in Fig. 1. We expect effect from that graphs that arise from the possible decays of  $\sigma \rightarrow \pi\pi$ ,  $a_0 \rightarrow \eta\pi$  etc.

$V_{\text{db}}$  is the double-bubble part that receives a special treatment in the 2PPI formalism

$$\begin{aligned} V_{\text{db}}(M^2, \phi_0) = & - \left( \frac{\lambda_1}{4} + \frac{\lambda_2}{8} \right) (3 \Delta_\sigma^2 + 15 \Delta_\pi^2 + 6 \Delta_\sigma \Delta_\pi) \\ & - \left( \frac{\lambda_1}{4} + \frac{\lambda_2}{8} \right) (3 \Delta_\eta^2 + 15 \Delta_{a_0}^2 + 6 \Delta_\eta \Delta_{a_0}) \\ & - \left( \frac{\lambda_1}{2} + \frac{\lambda_2}{4} \right) \Delta_\sigma \Delta_\eta - 3 \left( \frac{\lambda_1}{2} + \frac{3}{4}\lambda_2 \right) \Delta_{a_0} \Delta_\sigma \\ & - 3 \left( \frac{\lambda_1}{2} + \frac{3}{4}\lambda_2 \right) \Delta_\pi \Delta_\eta - 3 \left( \frac{3}{2}\lambda_1 + \frac{7}{4}\lambda_2 \right) \Delta_{a_0} \Delta_\pi. \end{aligned} \quad (13)$$

Note that all quantities  $\Delta$  are explicit function of the mass matrix  $M^2$  and the condensate  $\phi_0$ . They are obtained via

$$\Delta_*(M^2, \phi_0) = 2 \frac{\partial}{\partial M_*^2} V_q(M^2, \phi_0) \quad (14)$$

where  $*$  stands for  $\sigma, a_0, \eta$  or  $\pi$  and  $M^2$  is a short-hand notation for all four masses.

## 2.4 Equations of motion

The mass gap equations in the 2PPI effective action formalism are given by

$$\frac{\partial V_{\text{eff}}}{\partial M_*^2} = 0 \quad \text{with} \quad * = \sigma, a_0, \eta, \pi$$

and read explicitly

$$\begin{aligned} M_\sigma^2 = & m^2 - c + 3 \left( \lambda_1 + \frac{\lambda_2}{2} \right) \phi_0^2 + 3 \left( \lambda_1 + \frac{\lambda}{2} \right) (\Delta_\sigma + \Delta_\pi) \\ & + 3 \left( \lambda_1 + \frac{3}{2} \lambda_2 \right) \Delta_{a_0} + \left( \lambda_1 + \frac{\lambda_2}{2} \right) \Delta_\eta \end{aligned} \quad (15a)$$

$$\begin{aligned} M_\pi^2 = & m^2 - c + \left( \lambda_1 + \frac{\lambda_2}{2} \right) \phi_0^2 + \left( \lambda_1 + \frac{\lambda}{2} \right) (\Delta_\sigma + 5 \Delta_\pi) \\ & + \left( \lambda_1 + \frac{3}{2} \lambda_2 \right) \Delta_\eta + \left( 3 \lambda_1 + \frac{7}{2} \lambda_2 \right) \Delta_{a_0} \end{aligned} \quad (15b)$$

$$\begin{aligned} M_\eta^2 = & m^2 + c + \left( \lambda_1 + \frac{\lambda_2}{2} \right) \phi_0^2 + \left( \lambda_1 + \frac{\lambda}{2} \right) 3 (\Delta_\eta + \Delta_{a_0}) \\ & + \left( \lambda_1 + \frac{\lambda_2}{2} \right) \Delta_\sigma + 3 \left( \lambda_1 + \frac{3}{2} \lambda_2 \right) \Delta_\pi \end{aligned} \quad (15c)$$

$$\begin{aligned} M_{a_0}^2 = & m^2 + c + \left( \lambda_1 + \frac{3}{2} \lambda_2 \right) \phi_0^2 + \left( \lambda_1 + \frac{\lambda}{2} \right) (\Delta_\eta + 5 \Delta_{a_0}) \\ & + \left( \lambda_1 + \frac{3}{2} \lambda_2 \right) \Delta_\sigma + \left( 3 \lambda_1 + \frac{7}{2} \lambda_2 \right) \Delta_\pi . \end{aligned} \quad (15d)$$

They are made such that they resemble those of the Hartree-Fock approximation with the decisive difference that here  $\Delta_*$  is not a single bubble but calculated from Eq. (14). Neglecting the sunsets contributions to  $V_q$  in Eq. (14) would reduce all quantum corrections to simple bubbles; in this way the HF approximation is regained. Solving Eqs. (15) for all four quantum corrections one finds an expression for each quantum correction in terms of all four masses and the condensate.

The equation of motion for the condensate

$$\frac{\partial}{\partial \phi_0} V_{\text{eff}}(M^2, \phi_0) = 0$$

can be put in a very easy form by simplifying  $V_{\text{db}}(M^2, \phi_0) + V_{\text{cl}}(\phi_0)$ :

$$h_0 = M_\sigma^2 \phi_0 - (2\lambda_1 + \lambda_2) \phi_0^3 + \frac{\partial}{\partial \phi_0} V_{\text{sunsets}} . \quad (16)$$

The reader is encouraged to check this equation in the HF approximation by comparing with the one in Ref. [14].

### 3 The $O(N)$ linear sigma model

#### 3.1 Lagrangian

The linear sigma model with an  $O(4)$  symmetry is obtained from the  $U(2)_V \times U(2)_A$  model in the limit of infinite anomaly  $c \rightarrow \infty$  with fixed  $m^2 - c \rightarrow m_{O(4)}^2$ . The masses of both  $\eta$  and  $a_0$  become infinite and thus these two mesons drop out of the spectrum. The coupling is renamed to  $\lambda \equiv (\lambda_1 + \frac{\lambda_2}{2})$ , and  $\sigma$  and the three pions now share one  $O(4)$  multiplet. Extending the isospin symmetry from four to  $N$  dimension we can now write down the well-known Lagrangian of the  $O(N)$  linear sigma model

$$\mathcal{L}[\Phi] = \frac{1}{2} (\partial_\mu \Phi_i)^2 - \frac{1}{2} m^2 \Phi_i^2 - \frac{\lambda}{4} (\Phi_i^2)^2 + h_i \Phi_i \quad \text{with } i = 1, \dots, N \quad (17)$$

which has been studied extensively [8, 18, 19, 20, 22, 23, 24, 25, 30]. In this article we will extend the analysis performed in an earlier publication [19] to the case of explicit symmetry breaking and realistic values of the parameters.

#### 3.2 Equations of motion

The equations of motion are obtained from the 2PPI effective potential where the vacuum expectation value is set to be

$$\langle \Phi_i \rangle = \phi_0 \delta_{0i} ,$$

so that the 2PPI effective action reads [19, 25]

$$\begin{aligned} V_{\text{eff}}(\phi_0; M_\sigma^2, M_\pi^2) = & \frac{1}{2} M_\sigma^2 \phi_0^2 - \frac{\lambda}{2} \phi_0^4 - h_0 \phi_0 + \frac{m^2}{2\lambda(N+2)} [M_\sigma^2 + (N-1)M_\pi^2] \\ & - \frac{1}{8\lambda(N+2)} \left[ (N+1) M_\sigma^4 + 3(N-1) M_\pi^4 \right. \\ & \left. - 2(N-1) M_\sigma^2 M_\pi^2 + 2N\lambda^2 m^4 \right] + V_q(\phi_0; M_\sigma^2, M_\pi^2) . \end{aligned} \quad (18)$$

The quantum corrections consist of the following one- and two-loop terms

$$\begin{aligned} V_q(\phi_0; M_\sigma^2, M_\pi^2) = & \frac{1}{2} \ln \det(\partial^2 + M_\sigma^2) + \frac{N-1}{2} \ln \det(\partial^2 + M_\pi^2) \\ & - \lambda^2 \phi_0^2 [3 S_{\sigma\sigma\sigma} + (N-1) S_{\sigma\pi\pi}] . \end{aligned} \quad (19)$$



The mass gap equations follow from the stationarity condition

$$\frac{\partial}{\partial M_i} V_{\text{eff}} = 0$$

and read

$$M_\sigma^2 = m^2 + 3\lambda\phi_0^2 + \lambda[3\Delta_\sigma + (N-1)\Delta_\pi] \quad (20a)$$

$$M_\pi^2 = m^2 + \lambda\phi_0^2 + \lambda[\Delta_\sigma + (N+1)\Delta_\pi] , \quad (20b)$$

where all quantum corrections  $\Delta$  are explicit functions of both the condensate  $\phi_0$  and the masses defined as

$$\Delta_i(M_\sigma, M_\pi; \phi_0) = 2 \frac{\partial V_q}{\partial M_i^2} .$$

The equation for the condensate has the same structure as the one in the  $U(2)_L \times U(2)_R$  model, Eq.(16),

$$h_0 = \{M_\sigma^2 - 2\lambda\phi_0^2 - 2\lambda^2[3S_{\sigma\sigma\sigma} + (N-1)S_{\sigma\pi\pi}]\} \phi_0 . \quad (21)$$

In the following we will only investigate the case  $N = 4$ .

## 4 Numerical Results

### 4.1 Parameter fixing and loop graphs at finite temperature

The parameters in both models are fixed such that at  $T = 0$  the values of all masses are equal to the values in the Particle Physics Booklet [40], cf. Table 1, where we choose the mass of the  $\sigma$  meson to be 600 MeV. The value of the condensate  $\phi_0$  is related to the mesons decay constants and determined by the PCAC (partial conservation of axial vector current) hypothesis

$$f_a = d_{aa0} \phi_0 \equiv \phi_0 .$$

This fixes the condensate to  $\phi_0 = f_\pi$  because  $d_{aa0} = 1$ , so all decay constants are the same. For the two models of this paper the fixing can be done in a unique way because there are as many equations of motion as parameters. At tree-level it could be done even in the chiral limit (with  $h_0$  fixed to zero) since the equation for the condensate coincides with the one for the pion mass. Problems occur if one wants to include terms that contain a renormalization scale because the temperature-dependence of the condensate and the masses is varying with the renormalization scale [18]. Furthermore, terms originating from renormalization can be such that the gap equations are not solvable above a certain temperature [22, 41, 42]. Lenaghan and Rischke [18] have also shown that, in the  $O(N)$  model, there is no qualitative difference whether one includes the finite renormalization terms or not. Furthermore, the system only gets an extra parameter and all quantities are dependent on this scale which makes the results somewhat arbitrary. In order to get rid of

this extra parameter we take the phenomenological approach proposed before [14, 15, 18] and set all finite terms arising from regularization equal to zero which makes all quantum corrections only play a rôle at finite temperature. The resulting parameters can be found in Tables 2 and 3.

We postpone a scaling analysis of all parameters to another publication where we will also discuss parameter fixing with respect to the external masses derived from a 1PI effective action [43]. This will also solve the problem of the violation of Goldstone's theorem in the HF and two-loop 2PPI approximations (see, *e.g.*, Refs. [19, 25]).

Neglecting renormalization terms, the one-loop graphs at finite temperature — the boson determinant in the effective action and the single bubble (or tadpole)  $\mathcal{B}$  — are given by the following equations [19]

$$\ln \det(\partial^2 + M_i^2) = \frac{T}{\pi^2} \int_0^\infty dp \, \mathbf{p}^2 \ln [1 - e^{-E(\mathbf{p})/T}] \quad (22a)$$

$$\mathcal{B}_i = \frac{\partial}{\partial M_i^2} \ln \det(\partial^2 + M_i^2) = \frac{1}{2\pi^2} \int_0^\infty dp \, \frac{\mathbf{p}^2}{E_i(\mathbf{p})} n_i(\mathbf{p}) , \quad (22b)$$

where  $E_i(\mathbf{p}) = \sqrt{\mathbf{p}^2 + M_i^2}$  and

$$n_i(\mathbf{p}) = \frac{1}{e^{E_i(\mathbf{p})/T} - 1} \quad (23)$$

is the Bose-Einstein distribution. The sunset graph with three different masses  $M_i$ ,  $M_j$  and  $M_k$  is composed of three parts in each of which two of the three particles are taken from the heat bath

$$S_{ijk} = \mathcal{S}_{(ij)k}^{(2)} + \mathcal{S}_{(ki)j}^{(2)} + \mathcal{S}_{(jk)i}^{(2)} . \quad (24)$$

Here,  $\mathcal{S}_{(ij)k}^{(2)}$  is a sunset graph with  $i$  and  $j$  being thermal lines [19]

$$\mathcal{S}_{(ij)k}^{(2)} = \frac{1}{32\pi^4} \int_0^\infty dp_i dp_j \, \frac{p_i p_j}{E_i E_j} n_i(\mathbf{p}_i) n_i(\mathbf{p}_i) \ln \left| \frac{Y_{(ij)k}^+}{Y_{(ij)k}^-} \right| \quad (25)$$

with

$$Y_{(ij)k}^\pm = \left[ (E_i + E_j)^2 - (E_{(ij)k}^\pm)^2 \right] \cdot \left[ (E_i - E_j)^2 - (E_{(ij)k}^\pm)^2 \right]$$

and

$$E_{(ij)k}^\pm = \sqrt{(p_i \pm p_j)^2 + M_k^2} .$$

## 4.2 $O(N)$ model

For a given temperature  $T$  we first fix the value of  $\phi_0$  and then numerically extremize the effective potential in Eq. (18) with respect to  $M_\sigma$  and  $M_\pi$ . Thereby, we obtain a 1PI potential that is only a function of  $\phi_0$ . Using the equation of motion for the condensate (21)

particle	mass in MeV	
	with anomaly	without anomaly
$\sigma$	600	600
$\pi$	139.6	139.6
$a_0$	984.7	984.7
$\eta$	547.8	139.5

Table 1: Meson masses in the linear sigma models with and without axial anomaly. Note that, of course, there is no  $a_0$  and  $\eta$  meson in the  $O(4)$  model.

parameter	with anomaly	without anomaly
$m^2$	$-(103.78 \text{ MeV})^2$	$-(388.34 \text{ MeV})^2$
$c$	$(374.22 \text{ MeV})^2$	0
$h_0$	$(121.6 \text{ MeV})^3$	$(121.6 \text{ MeV})^3$
$\lambda_1$	-19.30	-35.70
$\lambda_2$	78.49	111.29
$\phi_0$	92.4 MeV	92.4 MeV

Table 2: Parameters in the  $U(2)_L \times U(2)_R$  model for masses as in Table 1.

parameter	ESB
$m^2$	$-(388.34 \text{ MeV})^2$
$h_0$	$(121.6 \text{ MeV})^3$
$\lambda$	19.94
$\phi_0$	92.4 MeV

Table 3: Parameters in the  $O(4)$  model for masses as in Table 1.

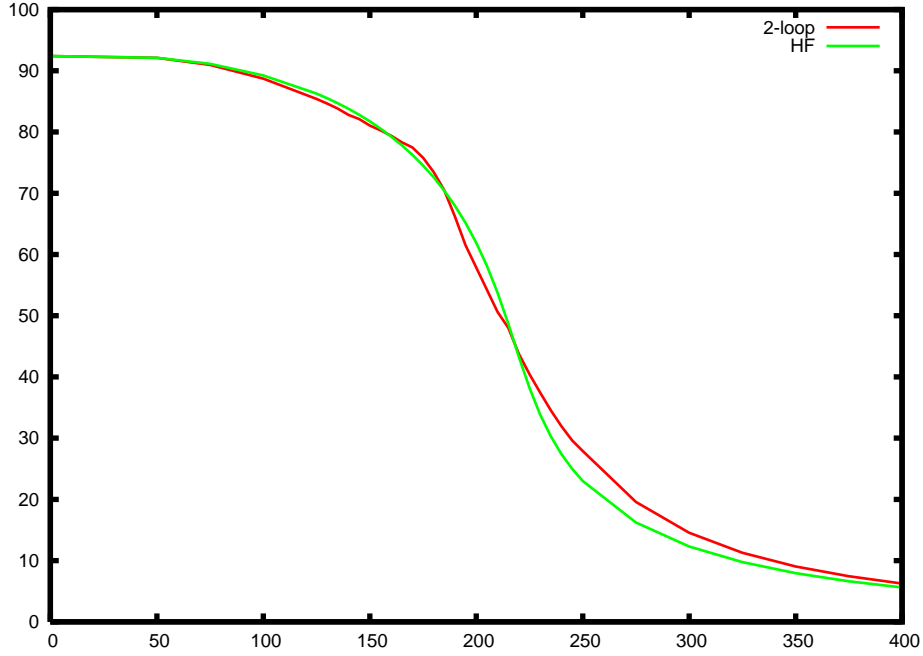


Figure 2: Temperature dependence of the condensate in the  $O(4)$  model. Comparison of the two-loop approximation (red line) with the HF approximation (green).

we eventually find the temperature-dependent value of the order parameter  $f_\pi(T)$ . This quantity is plotted in Fig. 2. There is no significant difference between the HF and the two-loop approximation. In the latter, the condensate drops faster at temperatures below 200 MeV and decreases more slowly for  $T > 250$  MeV than in the HF approximation.

The temperature dependence of the  $\sigma$  and pion mass is displayed in Fig. 3. The  $\sigma$  mass behaves similarly in both approximations while the pion mass first increases before it slightly drops at about  $T = 195$  MeV. Beyond temperatures of about 200 MeV the pion mass in both approximations is almost the same. In the vicinity of 300 MeV both masses become identical, a sign for the restoration of chiral symmetry. There, the temperature (to the third power) is equal to the value of the chiral quark condensate (see above).

### 4.3 $U(2)_L \times U(2)_R$ model

The procedure performed for the  $O(N)$  model, cf. Section 4.2, cannot be done for the  $U(2)_L \times U(2)_R$  model because it turns out that the potential  $V = V_{\text{cl}} + V_{\text{db}}$  has only a saddle point with respect to the four masses instead of a local extremum.

Solving the gap equations (15) is a cumbersome procedure because they contain derivatives of the sunset graph with respect to a mass. And in the vicinity of the decay threshold of the particles involved in a sunset graph, *e.g.*  $M_\sigma \simeq 2 M_\pi$ , the sign of the derivative of the sunset graph with respect to a mass quickly changes (see Fig. 4) which results in a

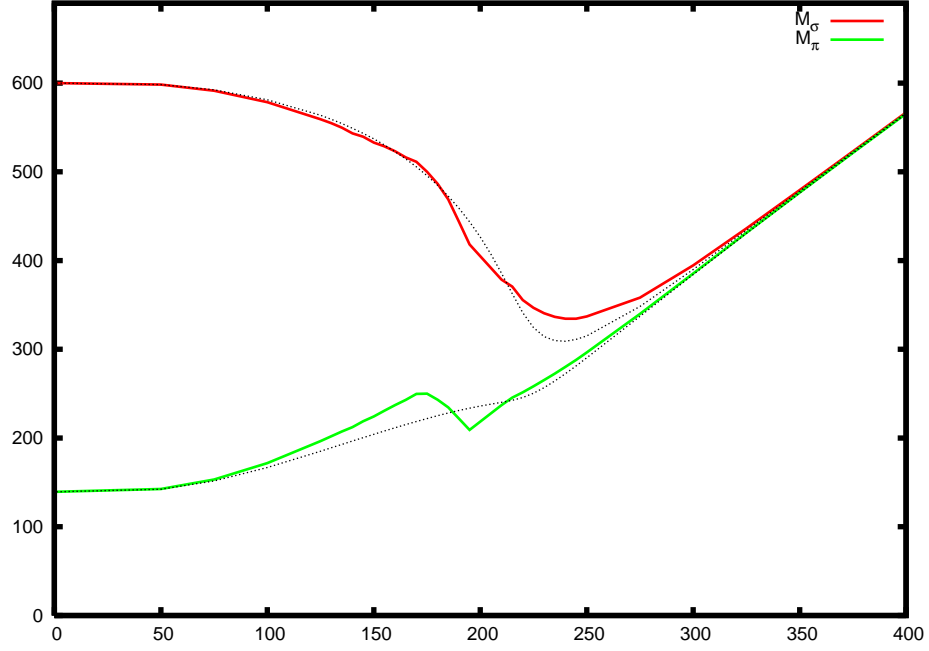


Figure 3: Temperature dependence of the masses in the  $O(4)$  model. Comparison of the two-loop approximation (solid lines) with HF (dotted).

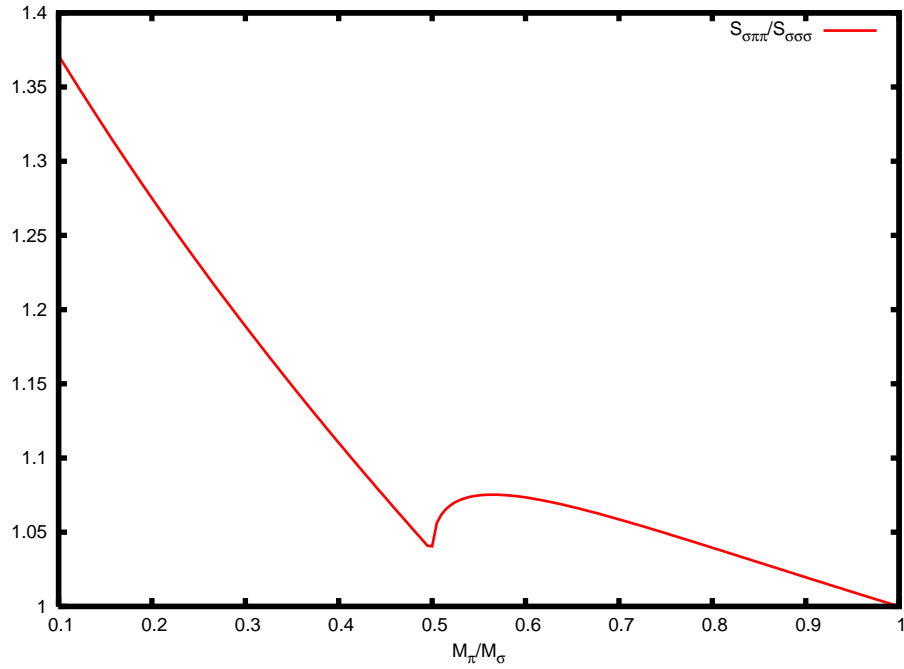


Figure 4: The ratio  $S_{\sigma\pi\pi}/S_{\sigma\sigma\sigma}$  at  $T = 150$  MeV.

numerically unstable behavior in this region. To avoid this trouble we solve the mass gap equations (15) in the HF approximation, *i.e.*, the quantum corrections  $\Delta$  to the masses only consist of single bubbles. We substitute these masses into the two-loop equation for the condensate (16) to obtain the temperature-dependent order parameter or decay constant  $f_\pi(T)$  and, for simplicity, call this approximation “two-loop” from now on.<sup>3</sup> In Fig. 5 we show this behavior for the  $U(2)_L \times U(2)_R$  model both with and without a  $U(1)_A$  anomaly. Compared to the HF approximation the order parameter decreases more slowly and exhibits some “bumps” in the curve. The reason for that behavior is a decay threshold effect caused by the sunset graphs [cf. Eq.(12)]. To check where the thresholds are crossed we plot the mass ratios for the decays  $\sigma \rightarrow \pi\pi$ ,  $a_0 \rightarrow \eta\pi$  and  $a_0 \rightarrow \eta\eta$  in Fig. 6. With an axial anomaly the curve of the order parameter in the two-loop approximation (see Fig. 5) deviates from the one of the HF approximation at a temperature of about 190 MeV. This is the region where the thresholds of the decays  $\sigma \rightarrow \pi\pi$  and  $a_0 \rightarrow \eta\pi$  are crossed (see Fig. 6). The sunsets become larger with rising temperature but also decrease with masses approaching the threshold from below. The latter behavior suddenly changes at the threshold and the sunsets suddenly grow which causes the immediate deviation from the HF results. Looking at the equation for the condensate (16) one can roughly conclude that a larger value of the condensate is needed to compensate for the contribution from the sunset terms.<sup>4</sup>

Without anomaly, the deviation from the HF approximation sets in at lower temperatures because the  $\sigma \rightarrow \eta\eta$  threshold is crossed already at temperatures about 100 MeV, followed by  $\sigma \rightarrow \pi\pi$  at about 175 MeV and, finally the on-shell decay  $a_0 \rightarrow \eta\pi$  becomes impossible at 200 MeV (see Fig. 6).

Comparing the prefactors of the different sunsets in Eq. (12), using the numerical values of the couplings from Table 2, we notice that, in the case of a finite  $U(1)_A$  anomaly, the contributions from  $S_{\sigma\eta\eta}$  and  $S_{a_0\eta\pi}$  are almost of the same size whereas  $S_{\sigma\pi\pi}$  is smaller by a factor of eight. So, the deviation from the HF approximation is dominated by a threshold effect of the decay  $a_0 \rightarrow \eta\pi$ . Without a  $U(1)$  anomaly the latter contribution even reduces to 7% of the size of the other two — always assuming that the contributions from all sunsets do not differ by orders of magnitude.

The temperature-dependent masses for the  $U(2)_L \times U(2)_R$  model with and without anomaly are displayed in Fig. 7. For a broken  $U(1)_A$  symmetry, especially the masses of the scalar mesons  $\sigma$  and  $a_0$  behave differently in the two-loop approximation than in HF whereas the masses of both pseudo-Goldstone bosons exhibit no qualitative difference in their temperature dependence between the two approximations. The observed deviations are due to the aforementioned threshold effects through sunset graphs. At a temperature of about 300 MeV the masses of the chiral partners become identical so that chiral symmetry is

---

<sup>3</sup>The same procedure in the  $O(N)$  model yields no significant difference to the HF approximation. There is a difference in the  $U(2)_L \times U(2)_R$  model because the coupling constants are larger by one order of magnitude, cf. Tables 2 and 3.

<sup>4</sup>This argument disregards the fact that all quantities in that equation depend on the condensate because we deal with a self-consistent resummation scheme.

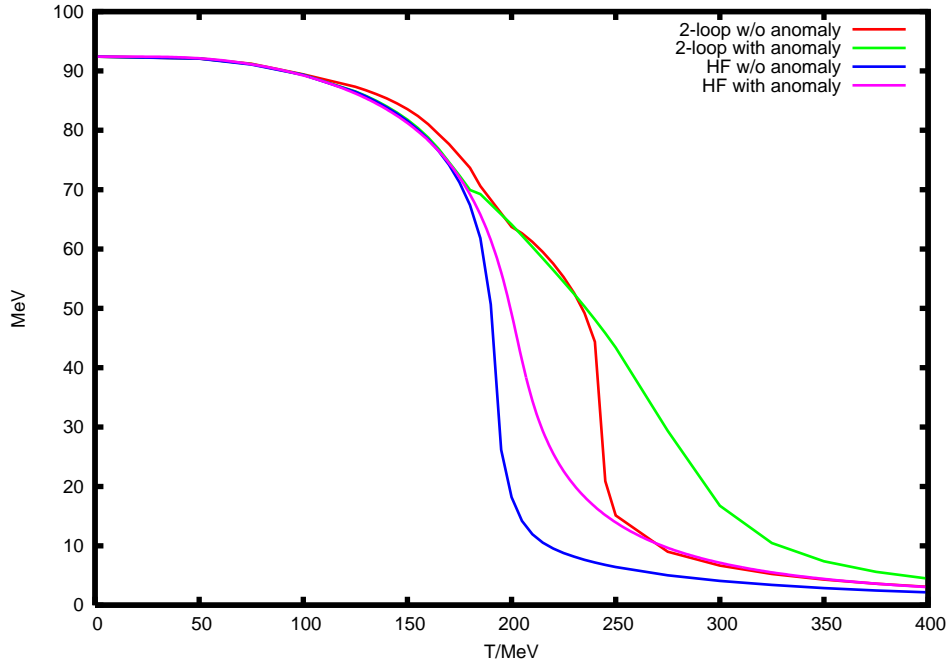


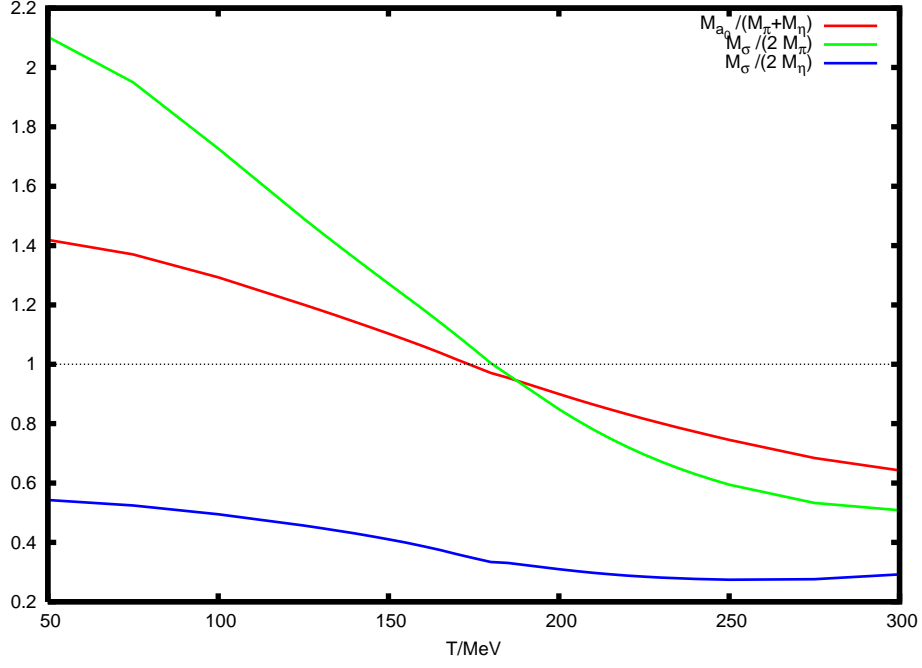
Figure 5: Temperature dependence of the condensate in the  $U(2) \times U(2)$  model. Comparison of the two-loop approximation (red and green line) with HF (blue and purple).

restored. The  $U(1)_A$  symmetry remains broken for the parameter  $c$  is not a function of temperature. The gap between the mass squares of the isospin partners  $\eta$  and  $\pi$  remains equal to  $2c$  according to Eq. (15).

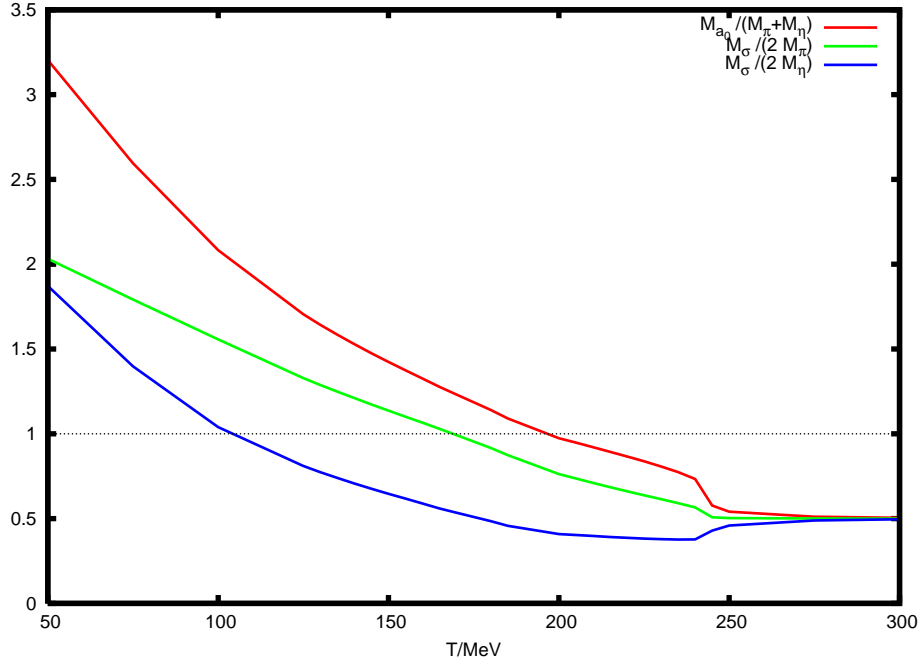
Without anomaly [see Fig.7(b)] the masses of the chiral partners tend to become identical at 240 MeV (200 MeV in HF) before the actual restoration of the full  $U(2)_L \times U(2)_R$  symmetry takes place at about 300 MeV. The sunset contributions seem to shift these points closer to one another. At finite temperature the mass of the  $\eta$  meson differs from the pion mass although they both started from 139.6 MeV at zero temperature. This indicates that the approximations considered in this article are not well-suited to model  $\eta$  as a fourth pseudo-Goldstone boson since they seem to contain an effective  $U(1)_A$  breaking through the unequal treatment of  $\eta$  and  $\pi$  in the gap equations (15). This phenomenon is comparable to the violation of Goldstone's theorem in the HF and two-loop approximation in the  $O(N)$  model [14, 19, 25].

There are indications from the lattice that at high temperatures the strength of the  $U(1)$  axial anomaly decreases [44]. We try to model this by fixing the parameters at zero temperature to the physical masses but considering the anomaly parameter  $c$  as a function of temperature. As an example we describe a suddenly dropping behavior at 175 MeV with the function

$$c(T) = c_0 \left[ \frac{1}{2} - \frac{1}{\pi} \arctan \left( \frac{T - T_A}{\Delta T} \right) \right] \quad (26)$$



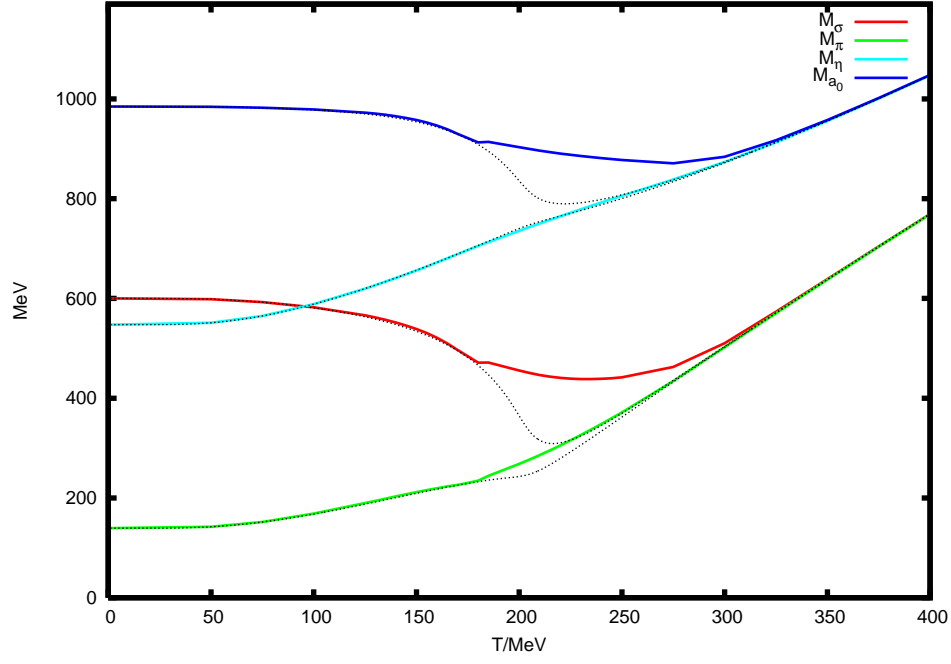
(a) with  $U(1)_A$  anomaly



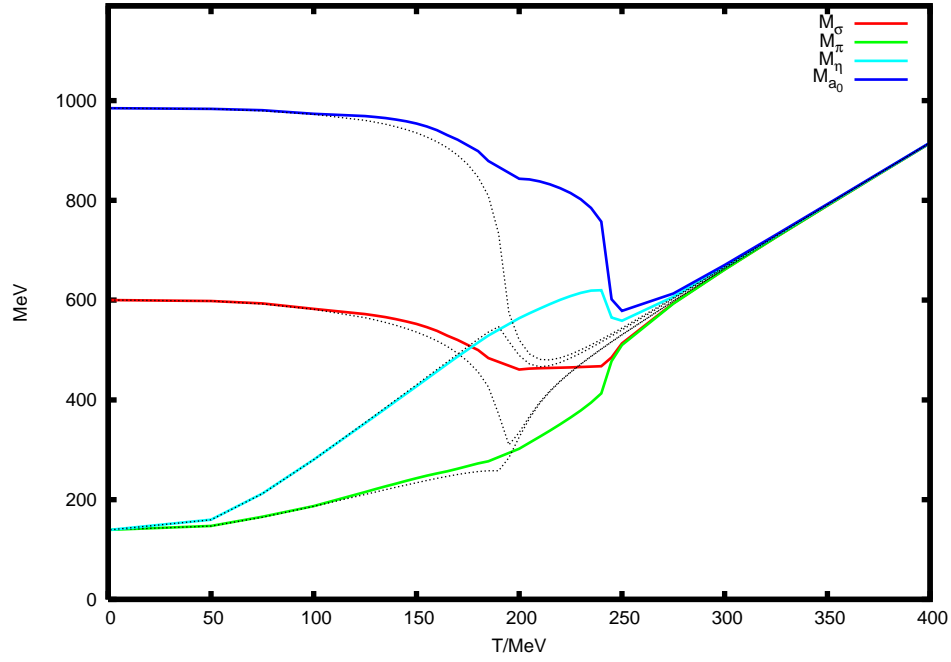
(b) without  $U(1)_A$  anomaly

Figure 6: Thresholds for the decays  $\sigma \rightarrow \pi\pi$ ,  $a_0 \rightarrow \eta\pi$  and  $\sigma \rightarrow \eta\eta$  in the  $U(2)_L \times U(2)_R$  model as functions of temperature.





(a) with  $U(1)_A$  anomaly



(b) without  $U(1)_A$  anomaly

Figure 7: Masses in the  $U(2) \times U(2)$  model as functions of temperature. Comparison of the 2-loop approximation (solid lines) with HF (dotted lines).

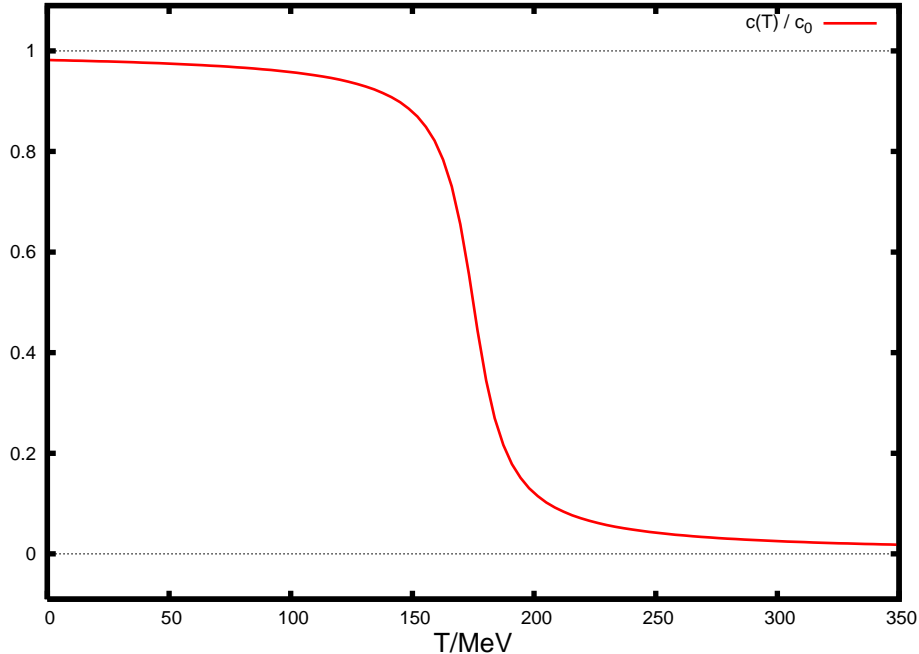


Figure 8: Modelled temperature dependence of the anomaly parameter  $c$ . The behavior is like the function in Eq. (26) with  $T_A = 175$  MeV and  $\Delta T = 10$  MeV.

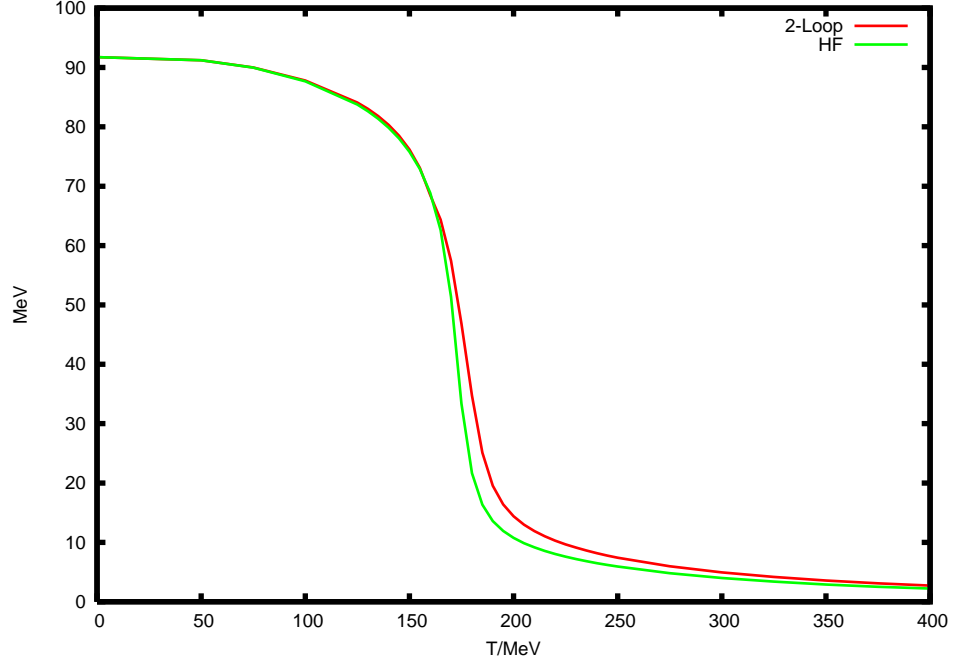
with  $T_A = 175$  MeV and  $\Delta T = 10$  MeV, see Fig. 8.

This causes a sharp decrease of the order parameter at about 175 MeV, cf. Fig. 9(a). The masses of the chiral partners become identical at about 190 MeV [see Fig. 9(b)]. Although the anomaly parameter tends to zero the full symmetry is only finally restored at about 300 MeV where all four masses become identical. The effect that a suddenly dropping anomaly parameter triggers the restoration of chiral symmetry was observed earlier in the linear sigma model with three quark flavors [16].

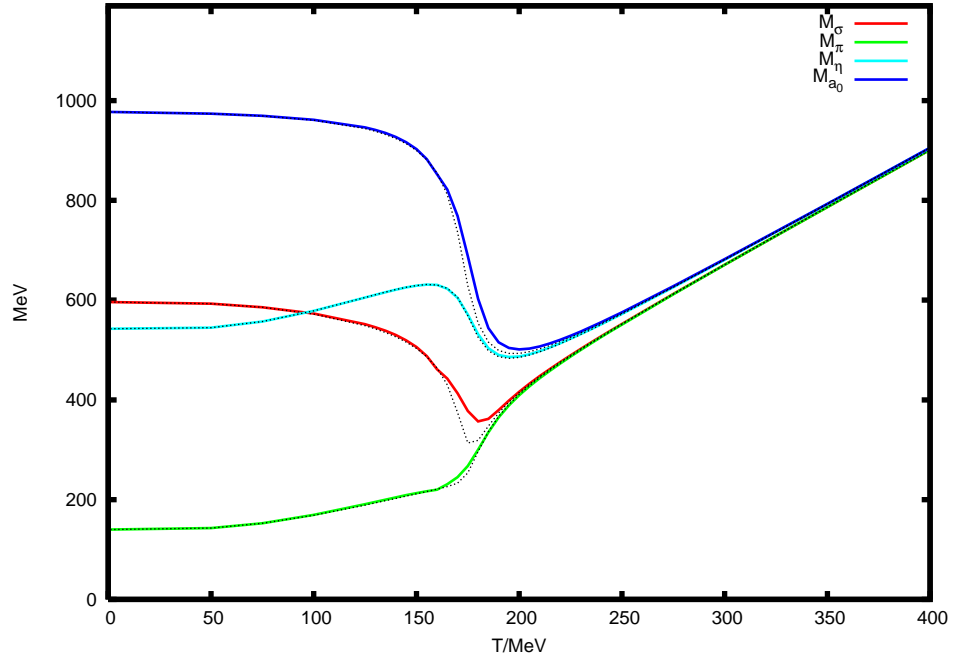
Varying  $\Delta T$  in Eq. (26) only makes the observables drop faster or more smoothly. Furthermore, the temperature region in which the condensate drops down and the masses of the chiral partners become identical is highly related to the temperature  $T_A$ ; with  $T_A = 150$  MeV, *e.g.*, chiral symmetry is restored at about 170 MeV but the full symmetry is, again, only restored at about 300 MeV.

## 5 Conclusions and outlook

We have investigated the restoration of chiral symmetry in the  $U(2)_L \times U(2)_R$  and in the  $O(N)$  linear sigma models at finite temperature. Taking into account two-loop sunset contributions makes the condensate drop less rapidly with increasing temperature; the crossover temperature increases from about 200 MeV in the HF approximation to about 250 MeV, or, equivalently, the restoration of chiral symmetry takes place at  $T \approx 300$  MeV



(a) Temperature dependence of the condensate.



(b) Temperature dependence of the masses in the two-loop approximation (solid lines) and in HF (dotted).

Figure 9:  $U(2)_L \times U(2)_R$  model with an anomaly parameter varying with  $T$ , see Fig.8.

instead of 250 MeV as in the HF approximation. The deviation from the HF approximation is induced by threshold effects especially of the decay  $a_0 \rightarrow \eta\pi$  which drive the value of the condensate away from zero. For a model with an axial  $U(1)$  anomaly the masses of the chiral partners become identical at about 300 MeV whereas a mass gap of  $2c$  between the isospin partners remains. But even with a zero anomaly parameter, there is an effective  $U(1)_A$  breaking by the approximation itself due to an unequal treatment of the  $\eta$  meson and the pions in the gap equations (15). Here as well, the sunset only rises the temperature where chiral symmetry is restored.

We have also investigated the effect of a temperature-dependent anomaly parameter  $c(T)$  as in Eq. (26). With a steep decrease at around 175 MeV we could reduce the crossover temperature below 200 MeV. In the chosen approximation, the masses of the chiral partners become identical at significantly lower temperatures (about 200 MeV) than with a fixed anomaly parameter. Nevertheless, the full symmetry is also only restored at about 300 MeV in this case. But a dropping anomaly parameter obviously triggers the restoration of chiral symmetry in the approximation we chose.

Comparing this work with recent publications one has to state that the effect of non-local corrections to the propagators, as in Refs. [26, 27], seems to be more efficient than considering only local corrections. Our approach is not able to reduce the crossover temperature significantly. So, it would be interesting to apply those methods also to the  $U(2)_L \times U(2)_R$  model.

Furthermore, the effective  $U(1)_A$  symmetry breaking that is inherent to the HF and two-loop approximation may be remedied by a different approximation, possibly by one inspired by a  $1/N$  expansion [43] similar to that used in Ref. [27].

Including strange mesons ( $N_f = 3$ ) could possibly lead to interesting non-linear effects since the  $U(1)_A$  anomaly term is trilinear for three flavors and thus would generate additional sunset graphs with different signs. Adding fermions (nucleons) to the model using a Yukawa coupling is also an attractive extension of this work. This has been done by several authors before [45, 46] but never beyond the level of one-loop.

## Acknowledgments

The author was supported by *Deutsche Forschungsgemeinschaft* as a member of *Graduiertenkolleg 841*. Part of this work was done during the *Marie Curie Doctoral Training Programme 2005* at ECT\* in Trento, Italy, which the author enjoyed very much.

## A Effective action of the $U(2)_L \times U(2)_R$ model

This Appendix contains details for the computation of the effective action of the  $U(2)_L \times U(2)_R$  model. We define the vacuum expectation value

$$\langle \Phi \rangle = T_a \phi_a$$

with a real-valued condensate  $\phi_0$  and shift the (complex)  $U(2)_L \times U(2)_R$  fields to

$$\Phi = \frac{1}{2}\phi_0 \mathbf{1} + T_a(\sigma_a + i\pi_a) ,$$

where  $\sigma_a$  and  $\pi_a$  are real and symbolize the scalar and pseudoscalar meson fields. The shifted Lagrangian is a sum of four parts,

$$\mathcal{L} = -V_{\text{class}} + \mathcal{L}_2 + \mathcal{L}_3 + \mathcal{L}_4 \quad (\text{A1})$$

The first part is the classical tree-level potential

$$V_{\text{class}}(\phi) = \frac{1}{2}m^2\phi_a^2 - 3\mathcal{G}_{ab} \phi_a\phi_b + \frac{1}{3}\mathcal{F}_{abcd} \phi_a\phi_b\phi_c\phi_d - h_a\phi_a , \quad (\text{A2})$$

the second part consists of all bilinear terms in the shifted fields

$$\begin{aligned} \mathcal{L}_2 = & \frac{1}{2}(\partial_\mu\sigma_a)^2 - \frac{1}{2} [m^2 \delta_{ab} - 6\mathcal{G}_{ab} + 4\mathcal{F}_{abcd} \phi_c\phi_d] \sigma_a\sigma_b \\ & + \frac{1}{2}(\partial_\mu\pi_a)^2 - \frac{1}{2} [m^2 \delta_{ab} + 6\mathcal{G}_{ab} + 4\mathcal{H}_{abcd} \phi_c\phi_d] \pi_a\pi_b , \end{aligned} \quad (\text{A3})$$

the third part contains trilinear terms describing the three-particle vertex

$$\mathcal{L}_3 = -\frac{4}{3}\mathcal{F}_{abcd} \phi_d\sigma_a\sigma_b\sigma_c - 4\mathcal{H}_{abcd} \phi_d\pi_a\pi_b\sigma_c , \quad (\text{A4})$$

and the last part contains the rest, *i.e.*, the four-vertex interactions,

$$\mathcal{L}_4 = -2\mathcal{H}_{abcd} \sigma_a\sigma_b\pi_c\pi_d - \frac{1}{3}\mathcal{F}_{abcd} (\sigma_a\sigma_b\sigma_c\sigma_d + \pi_a\pi_b\pi_c\pi_d) . \quad (\text{A5})$$

The structure of the mass matrices and interactions is given by the coefficients [14]

$$\mathcal{G}_{ab} = \frac{c}{6} (\delta_{a0}\delta_{b0} - \delta_{a1}\delta_{b1} - \delta_{a2}\delta_{b2} - \delta_{a3}\delta_{b3}) \quad (\text{A6a})$$

$$\begin{aligned} \mathcal{F}_{abcd} = & \frac{\lambda_1}{4} (\delta_{ab}\delta_{cd} + \delta_{ad}\delta_{bc} + \delta_{ac}\delta_{bd}) \\ & + \frac{\lambda_2}{8} (d_{abn}d_{ncd} + d_{adn}d_{nbc} + d_{acn}d_{nbd}) \end{aligned} \quad (\text{A6b})$$

$$\mathcal{H}_{abcd} = \frac{\lambda_1}{4}\delta_{ab}\delta_{cd} + \frac{\lambda_2}{8} (d_{abn}d_{ncd} + f_{acn}f_{nbd} + f_{bcn}f_{nad}) . \quad (\text{A6c})$$

From the structure of  $\mathcal{L}_2$ , Eq.(A3), we see that the tree-level mass matrix is diagonal if the expectation value  $\phi_a$  has only one component, *e.g.*,  $\phi_a = \delta_{a0} \phi_0$ . So there is no mixing between scalar and pseudoscalar mesons. Consequently, we can write down the general structure of the two-particle point-irreducible (2PPI) effective potential

$$V_{\text{eff}} = V_{\text{class}} + 2\mathcal{H}_{abcd} \Delta_{ab}^S \Delta_{cd}^P + \mathcal{F}_{abcd} (\Delta_{ab}^S \Delta_{cd}^S + \Delta_{ab}^P \Delta_{cd}^P) + V_q^{2\text{PPI}} , \quad (\text{A7})$$

where

$$\Delta_{ab}^S = \langle \sigma_a \sigma_b \rangle \quad \text{and} \quad \Delta_{ab}^P = \langle \pi_a \pi_b \rangle \quad (\text{A8})$$

denote expectation values of *local* composite operators and  $V_q^{2\text{PPI}}$  contains higher-order corrections made of 2PPI graphs. For the masses are diagonal those expectation values are diagonal as well,  $\Delta_{ab} \sim \delta_{ab}$ . Using the physical identification of the meson fields as given in Eq. (6) we declare

$$\Delta_\sigma \equiv \Delta_{00}^S \quad \Delta_\eta \equiv \Delta_{00}^P \quad (\text{A9a})$$

$$\Delta_{a0} \equiv \Delta_{11}^S = \Delta_{22}^S = \Delta_{33}^S \quad \Delta_\pi \equiv \Delta_{11}^P = \Delta_{22}^P = \Delta_{33}^P \quad . \quad (\text{A9b})$$

Contracting the coefficients  $\mathcal{F}_{abcd}$  and  $\mathcal{H}_{abcd}$  with the appropriate expectation values we obtain the following expression for the 2PPI effective action

$$\begin{aligned} V_{\text{eff}} = & V_{\text{class}} + V_q^{2\text{PPI}} \\ & - \left( \frac{\lambda_1}{4} + \frac{\lambda_2}{8} \right) (3 \Delta_\sigma^2 + 15 \Delta_\pi^2 + 6 \Delta_\sigma \Delta_\pi) \\ & - \left( \frac{\lambda_1}{4} + \frac{\lambda_2}{8} \right) (3 \Delta_\eta^2 + 15 \Delta_{a0}^2 + 6 \Delta_\eta \Delta_{a0}) \\ & - \left( \frac{\lambda_1}{2} + \frac{\lambda_2}{4} \right) \Delta_\sigma \Delta_\eta + 3 \left( \frac{\lambda_1}{2} + \frac{3}{4} \lambda_2 \right) \Delta_{a0} \Delta_\sigma \\ & - 3 \left( \frac{\lambda_1}{2} + \frac{3}{4} \lambda_2 \right) \Delta_\pi \Delta_\eta + 3 \left( \frac{3}{2} \lambda_1 + \frac{7}{4} \lambda_2 \right) \Delta_{a0} \Delta_\pi , \end{aligned} \quad (\text{A10})$$

where  $V_{\text{eff}}$  is a function of the condensate  $\phi_0$  and all four masses  $M_\sigma$ ,  $M_{a0}$ ,  $M_\eta$  and  $M_\pi$ . Note that this is the case for each quantity  $\Delta_*$  as well since it is given by Eq. (14).

## References

- [1] G. 't Hooft, Phys. Rev. Lett. **37**, 8 (1976).
- [2] G. 't Hooft, Phys. Rev. **D14**, 3432 (1976).
- [3] R. D. Pisarski and F. Wilczek, Phys. Rev. **D29**, 338 (1984).
- [4] F. Karsch, Lect. Notes Phys. **583**, 209 (2002), [hep-lat/0106019].
- [5] Z. Fodor and S. D. Katz, JHEP **04**, 050 (2004), [hep-lat/0402006].
- [6] P. de Forcrand and O. Philipsen, Nucl. Phys. **B642**, 290 (2002), [hep-lat/0205016].
- [7] M. Gell-Mann and M. Levy, Nuovo Cim. **16**, 705 (1960).
- [8] L. Dolan and R. Jackiw, Phys. Rev. **D9**, 3320 (1974).

- [9] E. Braaten and R. D. Pisarski, Phys. Rev. Lett. **64**, 1338 (1990).
- [10] E. Braaten and R. D. Pisarski, Nucl. Phys. **B337**, 569 (1990).
- [11] R. R. Parwani, Phys. Rev. **D45**, 4695 (1992), [hep-ph/9204216].
- [12] H. Verschelde and M. Coppins, Phys. Lett. **B287**, 133 (1992).
- [13] J. M. Cornwall, R. Jackiw and E. Tomboulis, Phys. Rev. **D10**, 2428 (1974).
- [14] D. Röder, J. Ruppert and D. H. Rischke, Phys. Rev. **D68**, 016003 (2003), [nucl-th/0301085].
- [15] J. T. Lenaghan, D. H. Rischke and J. Schaffner-Bielich, Phys. Rev. **D62**, 085008 (2000), [nucl-th/0004006].
- [16] J. Schaffner-Bielich, Phys. Rev. Lett. **84**, 3261 (2000), [hep-ph/9906361].
- [17] H. B. Geddes, Phys. Rev. **D21**, 278 (1980).
- [18] J. T. Lenaghan and D. H. Rischke, J. Phys. **G26**, 431 (2000), [nucl-th/9901049].
- [19] J. Baacke and S. Michalski, Phys. Rev. **D67**, 085006 (2003), [hep-ph/0210060].
- [20] N. Petropoulos, J. Phys. **G25**, 2225 (1999), [hep-ph/9807331].
- [21] A. Patkós, Z. Szép and P. Szépfalusy, Phys. Lett. **B537**, 77 (2002), [hep-ph/0202261].
- [22] S. Chiku and T. Hatsuda, Phys. Rev. **D58**, 076001 (1998), [hep-ph/9803226].
- [23] Y. Nemoto, K. Naito and M. Oka, Eur. Phys. J. **A9**, 245 (2000), [hep-ph/9911431].
- [24] G. Smet, T. Vanzielighem, K. van Acoleyen and H. Verschelde, Phys. Rev. **D65**, 045015 (2002), [hep-th/0108163].
- [25] H. Verschelde and J. De Pessemier, Eur. Phys. J. **C22**, 771 (2002), [hep-th/0009241].
- [26] D. Röder, J. Ruppert and D. H. Rischke, hep-ph/0503042.
- [27] D. Röder, hep-ph/0509232.
- [28] J. Baacke and S. Michalski, hep-ph/0409153.
- [29] J. Baacke and S. Michalski, Phys. Rev. **D70**, 085002 (2004), [hep-ph/0407152].
- [30] J. O. Andersen, D. Boer and H. J. Warringa, Phys. Rev. **D70**, 116007 (2004), [hep-ph/0408033].
- [31] H. van Hees and J. Knoll, Phys. Rev. **D65**, 025010 (2002), [hep-ph/0107200].

- [32] H. van Hees and J. Knoll, Phys. Rev. **D65**, 105005 (2002), [hep-ph/0111193].
- [33] H. van Hees and J. Knoll, Phys. Rev. **D66**, 025028 (2002), [hep-ph/0203008].
- [34] J. Berges, S. Borsányi, U. Reinosa and J. Serreau, Phys. Rev. **D71**, 105004 (2005), [hep-ph/0409123].
- [35] J.-P. Blaizot, E. Iancu and U. Reinosa, Nucl. Phys. **A736**, 149 (2004), [hep-ph/0312085].
- [36] Y. B. Ivanov, F. Riek, H. van Hees and J. Knoll, Phys. Rev. **D72**, 036008 (2005), [hep-ph/0506157].
- [37] C. Destri and A. Sartirana, hep-ph/0509032.
- [38] C. Destri and A. Sartirana, Phys. Rev. **D72**, 065003 (2005), [hep-ph/0504029].
- [39] C. Vafa and E. Witten, Nucl. Phys. **B234**, 173 (1984).
- [40] Particle Data Group, S. Eidelman *et al.*, Phys. Lett. **B592**, 1 (2004).
- [41] G. Baym and G. Grinstein, Phys. Rev. **D15**, 2897 (1977).
- [42] W. A. Bardeen and M. Moshe, Phys. Rev. **D34**, 1229 (1986).
- [43] S. Michalski, (2006), in preparation.
- [44] B. Allés, M. D’Elia and A. Di Giacomo, Nucl. Phys. **B494**, 281 (1997), [hep-lat/9605013], Erratum-ibid. **B679**, 397 (2004).
- [45] H.-S. Roh and T. Matsui, Eur. Phys. J. **A1**, 205 (1998), [nucl-th/9611050].
- [46] Á. Mócsy, I. N. Mishustin and P. J. Ellis, Phys. Rev. **C70**, 015204 (2004), [nucl-th/0402070].